After additional stirring for 1.5 hr at room temperature, excess sodium bisulfite was added. Ether (15 ml) was added to the reaction mixture and the phases were separated. The aqueous phase was extracted several times with ether. The combined ether phases were washed with 20% aqueous potassium carbonate solution, dried, and evaporated to give 600 mg of a soft solid. This was sublimed to give 360 mg (37%) of a colorless solid; a small portion was purified by glpc for analysis: mp 108–110° (sealed capillary); nmr (CCl_4) τ 3.79 (m, 2, vinyl), 7.32 (m, 2, bridgehead), 7.8–8.7 (m, 6, $(CH_2)_3$); ir (CCl_4) 1767 cm^{-1} (C=O).

Anal. Calcd for $C_8H_{10}O$: C, 78.65; H, 8.25. Found: C, 78.84; H, 8.37.

Acknowledgment. This work was supported in part by a grant from the Petroleum Research Fund of the American Chemical Society.

Studies of the Chymotrypsinogen Family. XII. "A" Type Substates of α-Chymotrypsin at Neutral and Alkaline pH Values[1]

Yung Dai Kim and Rufus Lumry*

Contribution from the Laboratory for Biophysical Chemistry, Chemistry Department University of Minnesota, Minneapolis, Minnesota 55455. *Received April 14, 1970*

Abstract: Time-dependent changes in the yield of indole fluorescence from α-chymotrypsin (α-CT) have been analyzed to show the existence of new substates of the best-folded state (state A) in the pH region from 7 to 10. Temperature studies provide values for enthalpy and entropy changes which characterize the interconversions of the substates. The slow processes produced by pH change at alkaline pH values are not accompanied by large changes in the latter quantities. These processes are partially controlled by two acid groups which become deprotonated cooperatively at about pH 9. Thermodynamic and rate information is provided for these processes and estimates of the contributions to the enthalpy and entropy changes from the protein–water subsystem and the protolysis groups are made. Near pH 8 there is a temperature-dependent process between substates A_bH_2 and A_fH_2 with relatively large enthalpy and entropy changes. This process, which has a half-conversion temperature of about 25°, has been shown to be of the two-state type and it has the characteristics which might be expected for a conformation change of considerable size. δ-Chymotrypsin shows similar substate versatility whereas chymotrypsinogen A and catalytically inactive derivatives of α-CT demonstrate no pH dependence of the fluorescence. In the alkaline pH region the substate behavior of δ-CT was similar to that of α-CT but was more closely first order in hydrogen ion activity than second order. As a general rule changes in ORD, fluorescence, and catalytic activity with pH are closely correlated.

The behavior of α-chymotrypsin (α-CT) above pH 7.5 reveals a variety of interesting features which have already proved to be of value in detecting structural variations participating in the catalytic process of this enzyme.[2–9] As judged by studies with "good" ester substrates, the protein is maximally active in the region from about pH 7 to about pH 8. K_m has its minimum values and the maximum velocity parameter, V_{max}, achieves its highest values in this region. Although V_{max} remains substantially constant with some ester substrates up to about pH 10, K_m increases with an apparent pK_a value of approximately 9.[2,9] This decrease has been shown to measure the change from a state of strong affinity for substrates and competitive inhibitors to a state of lower affinity. The number and characteristics of the acidic and basic groups which participate in chymotryptic catalysis have not been established. Different authors have used different substrates, different experimental conditions, and different postulated mechanisms in analyzing their data.

Studies of the behavior of α-CT at alkaline pH values by physical methods also have not led to firm conclusions. The optical rotation was first shown by Rupley, Dreyer, and Neurath[10] to be pH dependent. Hess and coworkers[11] and Parker and Lumry[12,13] extended these studies to include the dispersion of optical rotation of the protein and several of its derivatives. Both optical rotation and optical rotatory dispersion demonstrated pH-dependent behavior in the region from pH 8 to 10.

Parker and Lumry were hesitant about attributing their ORD observations to a change in protein conformation. Hess and coworkers[5–7,11] were less so and since then have provided a considerable body of additional evidence to support their contention that the pH-

(1) The work in this paper is from the Ph.D. Dissertation of Yung Dai Kim, University of Minnesota, 1968; the results were presented at the 154th National Meeting of the American Chemical Society, Chicago, Ill., 1967. This work was supported by the National Science Foundation, Grant No. GB7896, and Atomic Energy Commission, Grant No. AT(11-1)-894. This is paper No. 57 from this laboratory. Please request reprint by this number.

(2) A. Himoe, P. C. Parks, and G. P. Hess, *J. Biol. Chem.*, **242**, 919 (1967).

(3) M. L. Bender and F. C. Wedler, *J. Amer. Chem. Soc.*, **89**, 3052 (1967).

(4) W. K. Canady and K. J. Laidler, *Can. J. Chem.*, **36**, 1289 (1958).

(5) H. L. Oppenheimer, B. Labousse, and G. P. Hess, *J. Biol. Chem.*, 241, 2720 (1966).

(6) A. Y. Moon, J. M. Sturtevant, and G. P. Hess, *ibid.*, 240, 4204 (1965).

(7) J. McConn, E. Ku, C. Odell, G. Czerlinski, and G. P. Hess, *Science*, 161, 274 (1968).

(8) F. C. Wedler and M. L. Bender, *J. Amer. Chem. Soc.*, 91, 3894 (1969).

(9) M. L. Bender, M. J. Gibian, and D. J. Whelan, *Proc. Nat. Acad. Sci. U. S.*, **56**, 833 (1966).

(10) J. Rupley, W. Dreyer, and H. Neurath, *Biochem. Biophys. Acta*, **18**, 162 (1955); H. Neurath, J. Rupley, and W. Dreyer, *Arch. Biochem. Biophys.*, **65**, 243 (1956).

(11) B. H. Havsteen and G. P. Hess, *J. Amer. Chem. Soc.*, **85**, 79 (1963); J. McConn, G. D. Fasman, and G. P. Hess, *J. Mol. Biol.*, 39, 551 (1969).

(12) H. Parker and R. Lumry, *J. Amer. Chem. Soc.*, **85**, 483 (1963).

(13) H. Parker, Ph.D. Dissertation, University of Minnesota, 1967.

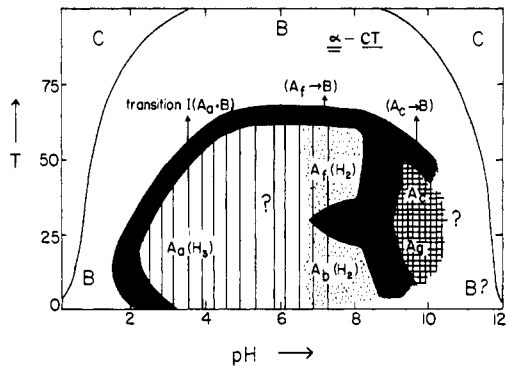

Figure 1. Semiquantitative state (or phase) diagram for α-CT. New states of α-CT identified in the present study are shown in addition to the pH-dependent and temperature-dependent changes in conformational states of α-CT included in the previous publication.[14] See ref 18 for a description of these diagrams.

dependent process in the alkaline region is indeed some form of conformation change. Biltonen, *et al.*,[14,15] and Parker and Lumry[12,13] demonstrated that the ORD spectrum was sensitive to pH, salt concentration, temperature, substrate, and inhibitor and postulated that their dependencies were associated with the making and breaking of an ion pair buried in the protein. Biltonen, *et al.*,[14,15] located the specific sensitivity in Cotton effects centered at 207 and 228 nm and attributed their local Cotton effects to unusual perturbations of single side-chain chromophores. More recently, Volini and Tobias[16] reported a pH-dependent variation of the ellipticities in circular dichroic bands at 229 and 202 nm. However, none of the data thus far presented need be interpreted as positive proof of a conformation change even if there were at present a generally accepted definition of that term. As most commonly used, the term "conformational change" is applied to a process in which the change in one or more physical observables is so large as to suggest that the alteration in the protein involves more than a few amino acid residues in an isolated area. A strictly geometric definition of the term, if possible, might have more utility, but for quantitative purposes the term must be defined in the conventional language of thermodynamics. Of the several possible thermodynamic quantities which might serve as a basis for a quantitative definition, the entropy is as convenient as any and is attractive because folding and unfolding processes are accompanied by large entropy changes. As is discussed elsewhere[17,18] for folding and unfolding processes of proteins we can use the temperature-independent entropy change as a criterion of size in conformation changes and with this choice, the definition has considerable merit relative to other alternatives though it is far from satisfactory on an absolute scale.

With the entropy criterion as our guide we have investigated several pH-dependent processes of α-CT at alkaline pH values which occur in the absence of substrates and inhibitors. For bookkeeping purposes the several thermodynamically distinct forms of α-CT which are now tentatively recognized as distinct species are shown on the state diagram in Figure 1. On comparison with the first version of this diagram[15] it can be seen that two new species A_bH_2 and A_fH_2 have been recognized as taking the place of a single fully-active, neutral-pH form previously called A_b (see also ref 18). A_b itself takes on new meaning as a metastable intermediate lying between the stable states (A_bH_2 + A_fH_2) and A_c, an alkaline species. We shall now present the evidence leading to this new detail in the state diagram.

Experimental Section

α-Chymotrypsin. Salt-free, three-times crystallized α-CT was obtained from Worthington Biochemical Co. The α-CT samples were purified by gel filtration on a column of G-25 (fine) Sephadex as previously described by Yapel, *et al.*[19] The purified solutions were used as a 1% stock solution directly, or lyophylized and stored at 4° for a few days before use. It proved to be essential for all the experiments to use α-CT thus purified in order to obtain reproducible results. The solution concentrations were measured spectrophotometrically on a Cary 15 recording spectrophotometer using the extinction coefficient of E_{282} = 2.03 l. g^{-1} cm^{-1} and assuming a molecular weight of 25,000 for α-CT. The pH values of protein solutions were maintained in the range 4–6 where the rate of autolysis of α-CT was relatively low. A stock solution of the purified enzyme was never kept for over 10 days at 4°. Older solutions gave highly erratic results.

Chymotrypsinogen A (CGN A), δ-Chymotrypsin (δ-CT), and γ-Chymotrypsin (γ-CT). Three times crystallized salt-free chymotrypsinogen A, two times crystallized salt-free γ-chymotrypsin, and salt-free lyophylized δ-chymotrypsin were purchased from Worthington Biochemical Co. and used after the same purification procedure as described for α-CT.

Diisopropylphosphoryl-α-chymotrypsin (DIP-CT), diphenylcarbamyl-α-chymotrypsin (DPC-CT), and succinylated α-chymotrypsin (Succ-α-CT) were kindly provided by Dr. D. F. Shiao. DIP-CT and DPC-CT were completely inactive acyl derivatives of α-chymotrypsin. Succ-α-CT was prepared by treating succinic anhydride with α-CT until all titratable amino groups in the enzyme molecule reacted to become succinylate ions. This derivative was known to be catalytically active when used with *N*-acetyl-L-tryptophan ethyl ester as substrate.[20]

Reagents. Reagent grade sodium chloride from Allied Chemical Co. was used without further purification. Tris(hydroxymethylaminomethane) buffer was obtained from Sigma Chemical Co.

Stopped-Flow Apparatus. This apparatus was a modified version of the original double-mixer design of Gibson,[21] constructed using commercial components and designed so that the changes in absorbance and fluorescence intensity could be followed simultaneously using a dual-beam oscilloscope. Each of the two driving syringes was enclosed in a separately thermostated compartment, and the temperature of each solution was measured with a thermistor inserted into the chamber. All six sides of the observation chamber were covered externally with Teflon walls of 2-mm thickness leaving openings for the windows. Regulation of the chamber temperature was achieved by circulating water from the thermostat through the baffled spaces between the stainless-steel block and the Teflon walls. Double quartz windows were installed to minimize heat exchange with the surroundings. The light source was either an HBO 100/2 Hg lamp (Osram Company), or a Type 110 Hg lamp (Illumination Industries Inc.). For fluorescence work a piece of glass which absorbed all the ultraviolet exciting beam and fluorescence below 312 nm was placed in front of the detecting photomultiplier tube.

A typical experiment with the stopped-flow apparatus was carried out in the following way. The system was held at a desired temperature within ±0.1° by circulating water maintained at that temperature. A buffered protein solution was made in 0.2 *M* sodium chloride and 0.02 *M* Tris–HCl buffer. When it was in-

(14) R. Biltonen, R. Lumry, V. Madison, and H. Parker, *Proc. Nat. Acad. Sci. U. S.*, 54, 1018 (1965).
(15) R. Biltonen, R. Lumry, V. Madison, and H. Parker, *ibid.*, 54, 1412 (1965).
(16) M. Volini and P. Tobias, *J. Biol. Chem.*, 244, 5105 (1969).
(17) J. Brandts, *J. Amer. Chem. Soc.*, 86, 4302 (1964).
(18) R. Lumry and R. Biltonen in "Structure and Stability of Biological Macromolecules," S. Timasheff and F. Fasman, Ed., Marcel Dekker, New York, N. Y., 1969.
(19) A. Yapel, M. Han, R. Lumry, A. Rosenberg, and D. Shiao, *J. Amer. Chem. Soc.*, 88, 2573 (1966).
(20) D. F. Shiao, R. Lumry, and J. Fahey, results from this laboratory, to be published.
(21) Q. Gibson in "International Colloquium on Rapid Mixing and Sampling Techniques Applicable to the Study of Biochemical Reactions," B. Chance, Ed., Academic Press, New York, N. Y., 1964.

tended to raise the pH of the protein system from the initial value of 8.0 to the final value of 9.0, the sample containing protein was adjusted to pH 8.0 and a solvent–buffer solution was adjusted to a predetermined pH value by adding small amounts of a 1 *M* solution of HCl or NaOH. A similar procedure was used when it was desired to start from a more alkaline protein solution and end at a less alkaline pH. After the solutions attained the desired thermal equilibrium in the driving syringes, they were mixed at a rate such that the experimental dead time was 10 msec.

Steady-State Fluorescence Experiments. A fluorimeter designed and constructed by Bednar and Biltonen[22] was used for the measurement of steady-state fluorescence yields. The cell compartment could be thermostated, and the fluorescence was detected at right angles to the direction of the excitation beam. The excitation band for these experiments was centered at 290 nm and had a bandwidth of 66 Å/mm. The bandwidth for the fluorescence detection at a slit width of 1 mm was 66 Å. The solutions used for the fluorimeter experiments on the pH dependence of the yield at 20° had the same compositions as the final reaction mixtures for the stopped-flow experiments. For each experiment on the protein sample the fluorescence of a sample of L-tryptophan in aqueous solution, at an optical density comparable to that of an α-CT sample at the wavelength of excitation, was measured to serve as the reference. Autolysis of α-CT at pH values above 6 was a very serious problem in steady-state experiments. The effect of protein autolysis on the fluorescence spectra of each sample was checked by observing the peak position and the yield of the fluorescence spectra on repeated scans. To be acceptable an experiment had to demonstrate no noticeable shift ($<\pm 1$ nm) in the wavelength of maximum fluorescence emission, 331 nm (after correction for the sensitivity of the monochromator and the photomultiplier tube). A slight red shift ($>\pm 1$ nm) in the peak position appeared when autolysis effects became significant.

Reproducibility of the fluorescence yields for a given sample was 1%, but, as yet not understood differences in mean steady-state fluorescence yields were observed on comparing different samples. This phenomenon is challenging since it demonstrates that the fluorescence yield is the most sensitive measure of the quality of α-CT which has been found in this laboratory.

Temperature-Dependent Change in Steady-State Fluorescence Yield of α-CT and CGN A at pH 8.0. For this series of experiments the protein concentrations used were 5–6 times lower than those for the isothermal experiments. The experiments were carried out at each temperature in such a way that the time taken for the completion of each experiment did not exceed 35 min. It was essential to repeat an experiment at a given temperature at least three times in order to ensure reproducibility. Calcium ions which are known to effect stabilization of α-CT molecules against autolysis at alkaline pH and high temperature were added to α-CT samples for several control experiments. The experiments with CGN A were carried out with one solution by varying the temperature of the system from 7 to 40°. In all cases, an L-tryptophan sample (pH 6.7) was run concurrently with the protein sample as a reference.

pH-Dependent Fluorescence Changes of Other Chymotrypsin Derivatives. The technique of the transient fluorescence experiment for α-CT was employed to investigate the fluorescence behavior of the zymogen and some other catalytically active and inactive chymotrypsin derivatives. Presence or absence of the fluorescence change with the variation of pH in the alkaline pH range could be checked easily under comparable experimental conditions by this technique.

Difference Spectra. The two samples compared in each case for isothermal difference spectra experiments were identical in protein and buffer concentration but different in pH. The reference state chosen was that at pH 8.0 throughout the experiments. For the temperature-dependent difference-spectra experiments, however, two samples that were identical in their composition and pH values were used. The reference temperature was 10° and the temperature of the sample cell was varied from 10 to 38°.

Optical Rotatory Dispersion Experiments. A Cary Model 60 recording spectropolarimeter was used with a 2.0-nm path-length quartz cell. The cell compartment was thermostated with a specially designed thermostating block. The experimental conditions were the same as for the pH-dependent fluorimeter experiments.

Sedimentation Experiments. A Spinco-Model E Analytical Ultracentrifuge equipped with Schlieren optics was used throughout the experiments. The standard analytical cells, one with an ordinary window and the other with a wedge window, were used for simultaneous experiments. A typical experiment employed a pair of samples whose compositions were initially identical but the pH value of one sample was adjusted to 8.0 and the other to 9.0.

Results

Transient Changes in Fluorescence Intensity for α-CT. A change in fluorescence intensity of the α-CT system with time as a result of a rapid pH change could be followed with the stopped-flow apparatus. In these experiments at $t = 0$ the pH of the protein solution was shifted either up or down the pH scale between 8 and 10. When the pH of the system was suddenly increased, the fluorescence intensity decreased with time, and the reverse situation was observed when the pH was shifted downward. The magnitude of the change was found to be dependent upon the pH, the protein concentration, and the temperature of the system. There was a single detectable relaxation transient for this process, and it gave first-order kinetics behavior regardless of the direction of pH change.

A series of experiments was carried out to check the respective dependence of the first-order rate constants on the initial pH and the final pH of the system at a given temperature. Table I illustrates the results of a typical set of these experiments. As shown in Table I, at a given temperature, the rate constant of the fluorescence change is independent of the initial pH of the system and depends only on the pH of the final state within experimental error. Furthermore, the rate is also independent of the protein concentration when all other conditions are held constant. The effect of Tris–HCl buffer on the transition was tested by using phosphate buffer in its place keeping all other conditions the same. The close agreement between the two experiments shows that the rate constants are independent of buffer type.

Table I. Dependence of the First-Order Rate Constants on the Hydrogen Ion, Buffer, and Protein Concentrations of the α-CT System[a]

Concn, α-CT, %	Buffer and salt, *M*	pH (initial)	pH (final)	Apparent rate constant, sec^{-1}
0.05	NaCl, 0.2	9.10	8.81	0.357 ± 0.015
	Tris–HCl, 0.02	8.50	8.80	0.378 ± 0.008
		8.00	8.81	0.373 ± 0.007
	NaCl, 0.2	8.00	8.41	0.306 ± 0.014
	Tris–HCl, 0.02	8.00	8.96	0.398 ± 0.004
		8.00	9.04	0.420 ± 0.023
	Phosphate ionic strength, 0.1	8.00	8.80	0.353 ± 0.015
0.075	NaCl, 0.2	8.00	8.81	0.372 ± 0.006
0.19	Tris–HCl, 0.02	8.00	8.71	0.321 ± 0.024

[a] Temperature for this set of experiments is 20.0 ± 0.1°. The errors shown here are the average errors among the duplicate experiments.

Four series of experiments were carried out under identical conditions except for variation in temperature. Considerable care was necessary to minimize the effect of autolysis since all the experiments were performed at high pH values where the rate of autolysis is high. In any given experiment the entire process from the time when pH values of the solutions were originally adjusted until the last picture was taken never exceeded 35 min.

(22) M. S. Walker, T. W. Bednar, and R. Lumry, *J. Chem. Phys.*, 47, 1020 (1967).

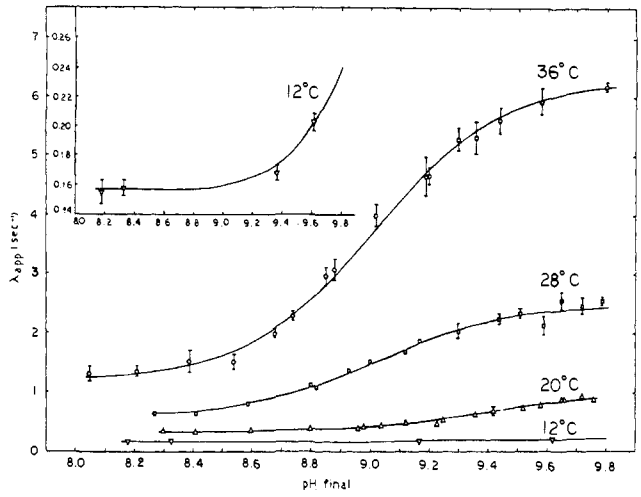

Figure 2. The observed apparent first-order rate constant for the transient fluorescence change of α-chymotrypsin as a function of pH and temperature: α-CT = 2×10^{-5} *M*; Tris-HCl buffer = 0.02 *M*; NaCl = 0.2 *M*. The theoretical curves at different temperatures are shown in solid lines.

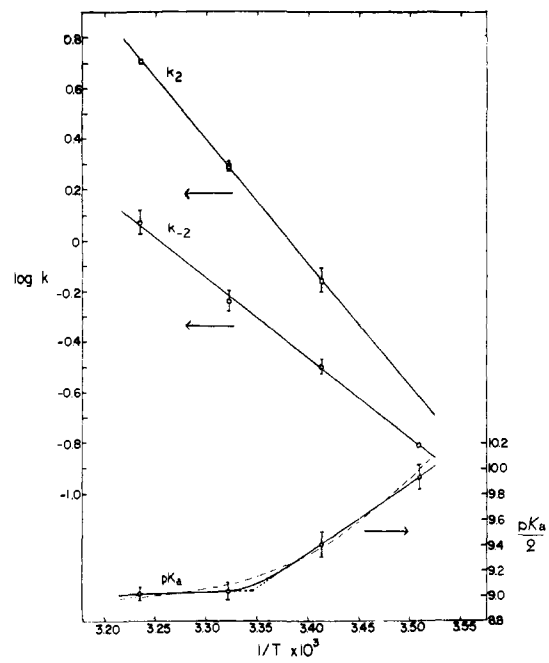

Figure 3. Arrhenius plots for the rate parameters evaluated from the theoretical analysis of Figure 2, and van't Hoff plot (in terms of pK_a *vs.* $1/T$). The estimates of the thermodynamic functions are based on the solid lines in the van't Hoff plot. One of the alternative curves through the points is shown with the dotted line.

A series of pictures taken for one experiment was then numbered and the calculated rate constants were checked in sequence so that any systematic error or autolysis effect could be detected. In all cases only small random deviations from the standard mean values were detected.

The highest pH value at which the experiments proved to be useful was 9.80. Above this pH value the quenching effect of phenolate ion on tryptophan fluorescence[23,24] became serious. Two consecutive relaxations, one fast decay in fluorescence intensity followed by a slow decay, appeared.

As shown in Figure 2 each set of the experimental points at a single temperature manifested the behavior required by eq 1 and 2 in which the first step, completed in less than 10 msec, is the ionization of two protonated groups in the catalytically active enzyme species (A_bH_2) that is predominant at pH 8, and the second step is the relatively slow process in which A_b comes into equilibrium with species A_c. The notations used here correspond to the definitions of Biltonen, *et al.*[14,18] The fast preequilibrium has an equilibrium constant $K_a = k_1/k_{-1}$. λ_{app} is the reciprocal of the experimental relaxation time and is equal to λ_2 derived in the Appendix. The constant K_a is the protolysis equilibrium constant but is somewhat unusual because this process releases two protons.

$$A_bH_2 \underset{k_{-1}}{\overset{k_1}{\rightleftharpoons}} A_b + 2H^+ \quad (1)$$

$$A_b \underset{k_{-2}}{\overset{k_2}{\rightleftharpoons}} A_c \quad (2)$$

$$\lambda_{app} = k_{-2} + \frac{k_2}{1 + \frac{[a_H]^2}{K_a}} \quad (3)$$

In Figure 2 the theoretical curves drawn through the experimental points are the results of a least-squares analysis based on eq 3. In these analyses for a given set of experimental values of λ_{app} at various pH values, the parameter K_a has been varied to yield a "best fit" of the experimental data to the equation and hence "best-fit" values of k_2 and k_{-2}. The results are summarized in Table II. The errors indicated for k_2, k_{-2} are the standard deviations from the "least-squares fit" of the data and those for pK_a are estimated from $\Sigma\chi^2$.

Table II. Rate Parameters and pK_a at Various Temperatures According to Mechanisms 1 and 2

Temp, °C	pK_{app}	k_2, sec^{-1}	k_{-2}, sec^{-1}
36	18.04 ± 0.10	5.129 ± 0.009	1.192 ± 0.133
28	18.08 ± 0.14	1.973 ± 0.103	0.582 ± 0.052
20	18.82 ± 0.20	0.703 ± 0.080	0.321 ± 0.022
12	19.84 ± 0.20[a]	0.242[a]	0.157 ± 0.002

[a] See text for the procedure of calculating pK_a and k_2 at 12°.

The Arrhenius plots and van't Hoff plot of the data from Table II are shown in Figure 3. The Arrhenius plots for k_2 and k_{-2} are linear within error.

A special situation arises when the temperature drops below 20° since the upper portion of the curve of Figure 2 at pH 9.8 cannot be measured due to the interference of quenching by phenolate ion in this region. Therefore, the following procedure was adopted to construct the theoretical curve at 12°: (a) the lower part of the curve can be studied in the same way as before since the curve levels off at relatively high pH. This lower limit of the full curve gives k_{-2} at 12°. The value so obtained fell precisely on the linearly extended Arrhenius plot for k_{-2}. (b) This behavior verifies the assumption that the k_{-2} process is the same at all experimental temperatures. It is therefore unlikely that k_2 at 12° lies off the k_2 Ar-

(23) S. Yanari, F. A. Bovey, and R. Lumry, Abstracts, 142nd National Meeting of the American Chemical Society, Atlantic City, N.J., Sept 1962, No. 7R-18.
(24) B. H. J. Bielski and S. Freed, *Anal. Biochem.*, 7, 192 (1964).

rhenius line. Hence, one may compute the value of k_2 at 12° from the extended straight line of its Arrhenius plot. (c) A point, λ_{app}, at pH 9.62 and 12° was very well established by repeating the same experiment several times. (d) Making use of these values of k_{-2}, k_2, and λ_{app} for 12° obtained in this way and eq 3, K_a is calculated on the assumption that the mechanism of eq 1 and 2 is still valid at this temperature. The complete van't Hoff plot for K_a including the computed 12° point is shown in Figure 3. The displacement of this point from the straight line will be discussed in the following section. The thermodynamic parameters corresponding to k_2 and k_{-2} are given in Table III.

Table III. Thermodynamic Functions for the Slow Equilibrium Step $A_b \rightleftharpoons A_c$, in Equations 1 and 2[a]

Type of transition	Properties: $\Delta H^{\pm}$, kcal/mol	$\Delta S^{\pm}$, eu/mol	$\Delta F^{\pm}$, kcal/mol
$A_b \xrightarrow{k_2} A_c$	21.7 ± 0.4	15.1 ± 1	17.3 ± 0.1
$A_c \xrightarrow{k_{-2}} A_b$	13.9 ± 0.5	−13 ± 2	17.9 ± 0.1
Type of equilibrium	**Properties: $\Delta H°$, kcal/mol**	**$\Delta S°$, eu/mol**	**$\Delta F°$, kcal/mol**
$A_b \rightleftharpoons A_c$	7.8 ± 0.6	28 ± 2	−0.6 ± 0.1

[a] The errors for $\Delta H^{\pm}$ are average errors estimated from the Arrhenius plots.

Steady-State Fluorescence Yield at Alkaline pH. The steady-state fluorescence yields were calculated from the ratio of the areas under the fluorescence spectra, one for α-CT and the other for the appropriate tryptophan reference sample. The relationship[25] used for the calculations was

$$Q = Q_{ref} x \left(\frac{A}{A_{ref}}\right)\left(\frac{I_{ref}}{I}\right)$$

in which A and A_{ref} are respective areas under the fluorescence bands of the protein and tryptophan sample and I and I_{ref} are absorbances of the protein and reference sample at the wavelength of excitation. The fluorescence yield at various pH values measured at 20° and calculated for $Q_{ref} = 1.00$ is shown in Figure 4. Despite the large errors (see Experimental Section), the statistical average of the experimental points significantly reveals the general picture of the change in fluorescence yield with pH in the range of interest.

Qualitatively, our results agree with those of previous workers in the pH range of 8.0–10.0 (Yanari, *et al.*,[23] and Bielski[24]); the fluorescence yield at 20° is highest near pH 8.0 and drops rapidly with increasing pH. Quantitative comparisons cannot be made since the yield was found to be extremely sensitive to the experimental conditions employed: purity of the enzyme, the type and concentration of salt and buffer, temperature, etc.[25]

From mechanisms 1 and 2 we can write eq 4 for the pH-dependent change in steady-state fluorescence yield.

$$Q = \frac{q_{A_bH_2}[a_H]^2 + q_{A_b}K_a + q_{A_c}(k_2/k_{-2})K_a}{K_a + [a_H]^2 + (k_2/k_{-2})K_a} \quad (4)$$

(25) Y. D. Kim, Dissertation, University of Minnesota, 1968.

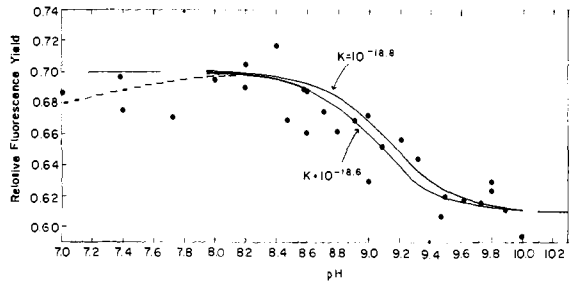

Figure 4. Relative fluorescence yield of α-chymotrypsin *vs.* pH value: α-CT = 2×10^{-5} *M*; Tris-HCl buffer = 0.02 *M*; at 20.0 ± 0.2°. The theoretical curves are calculated using the two extrapolated values shown at the pH values lower than 8.0 and higher than 10.0. Two curves are calculated assuming the pK_a values as 18.8 and 18.6, respectively.

Equation 4 yields three useful special cases (eq 5a–5c).

$$a_H \rightarrow 0;\ Q = \frac{q_{A_b} + (k_2/k_{-2})q_{A_c}}{1 + (k_2/k_{-2})} \quad (5a)$$

$$a_H^2 = K_a;\ Q = \frac{q_{A_bH_2} + q_{A_b} + (k_2/k_{-2})q_{A_c}}{2 + (k_2/k_{-2})} \quad (5b)$$

$$a_H \rightarrow \infty;\ Q = q_{A_bH_2} \quad (5c)$$

In eq 4 and 5 q_i denotes the intrinsic fluorescence yield for species i.

In order to establish the validity of eq 1 and 2 the steady-state fluorescence yield at various pH values was computed from this mechanism using the values of k_2 and k_{-2} obtained in the stopped-flow experiments, and the special cases of eq 4 given in eq 5. The values of parameter K_a are adjusted to achieve the "best-fit" of theoretical curves, as has been done for the transient study at 20°. Values of pK_a of 18.8 and 18.6 at 20° give equally good agreement and the errors are such that neither value can be said to be statistically more significant than the other. The best-fit value of pK_a in the stopped-flow experiments at 20° is 18.82. Thus the results are also consistent with mechanisms 1 and 2.

Other Physical Measurements on α-CT at Alkaline pH Values. Chymotrypsin is known to dimerize as well as to form higher aggregates in the pH range of these experiments. The release of two protons rather than one in the preequilibrium step of eq 1 might suggest that some of the processes detected in these experiments involve a change in state of aggregation. This possibility is inconsistent with the kinetics results but is nevertheless worth investigating. Velocity sedimentation experiments were carried out at pH 8.0 and 9.0 at 20° with varying protein concentration. The results are shown in Figure 5. At 0.05% there is negligible dimerization under any circumstances and the dimerization equilibrium is so far in favor of the monomeric species that concentrations at least twice this high could have been used without introducing complications from dimerization.

An attempt was made to relate the pH-dependent processes studied by fluorescence methods with the ORD observations of Parker and Lumry,[11] Hess and coworkers,[10] and Biltonen, *et al.*[13,14] This comparison was motivated by the indication that the ORD changes had a higher than first-order dependence on hydrogen-ion activity and by the proposal of Parker and Lumry that the ORD results might be a consequence of a buried ion

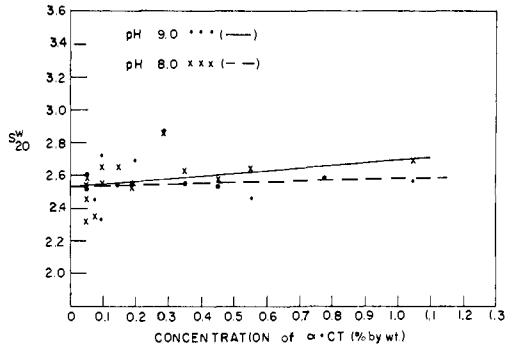

Figure 5. The velocity sedimentation coefficient as a function of α-CT concentration at pH 8.0 and 9.0: NaCl = 0.2 *M*; Tris-HCl buffer = 0.02 *M*; *T* = 20°.

pair. Experimentally we were able to observe the two Cotton effects reported by Biltonen, *et al.*, in the pH range from 8.0 to 10.0 using a sample at pH 8.0 as reference. Our ORD results were consistent with the analysis of these workers. Nonetheless, the magnitudes of the relative change in specific rotations were not large enough to allow any quantitative analysis of the results.

As a final test of pH behavior in the alkaline region the difference spectrum in the near ultraviolet was determined as a function of pH using a sample at pH 8.0 as reference. There was a significant change in the absorption spectrum of α-CT due to phenolate ionization with apparent pK_a greater than 10. It was not possible to separate out a similar contribution which could be attributed to the process of eq 1 and 2.

Fluorescence Behavior of Some Other Chymotrypsin Derivatives. A rough correlation among ORD behavior, catalytic activity, and fluorescence change is found with α-CT, δ-CT, CGN A, and three chemical derivatives of α-CT. The results shown in Table IV

Table IV. Correlations between Enzymic Activity, Optical Rotatory Dispersion, and Fluorescence Yield of CGN-A, α-CT, and Some Derivatives in the pH Range 8.0–9.5 and High Salt

	Properties		
Type of enzymes	Catalytic activity	ORD change with pH	Fluorescence change with pH
α-Chymotrypsin	Active	Yes	Yes
δ-Chymotrypsin	Active	Yes[b]	Yes
γ-Chymotrypsin	Active	Yes[b]	Yes
Succinylated-α-chymotrypsin	Active[a]	Yes[b]	Yes
Chymotrypsinogen-A	Inactive	No[c]	No
DIP-α-chymotrypsin	Inactive	No[c]	No
DPC-α-chymotrypsin	Inactive	No[c]	No

[a] 80% activity on the basis of 100% activity for the purified α-CT under comparable conditions. [b] D. F. Shiao, Dissertation, University of Minnesota, 1968. [c] References 12 and 13.

demonstrate the qualitative consistency obtained. They suggest that a common set of pH-dependent processes is responsible for the variations found with the three observations.

Temperature-Dependent Change in Protein Conformation at pH 8.0. The appearance of curvature in the

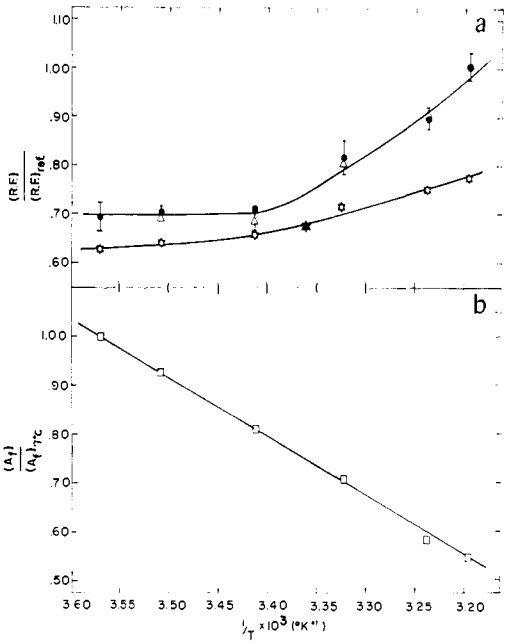

Figure 6. (a) Relative fluorescence yield of α-chymotrypsin and chymotrypsinogen *vs.* 1/*T*. α-CT = 4 × 10^{-6} *M*, Tris-HCl buffer = 0.02 *M*; -●-●-●, in 0.2 *M* NaCl; Δ-Δ-Δ-, in 0.1 *M* $CaCl_2$, at pH 8.00. CGN = 4 × 10^{-6} *M*, Tris-HCl buffer = 0.02 *M*, NaCl = 0.2 *M*, pH 8.00, ☆-☆. The temperature was raised from 7 to 40°. The filled point, ★, was obtained after the solution was cooled from 40 to 25°. The fluorescence of L-tryptophan in water at pH 6.7 was used as a reference, for which the value of 1.00 was assumed at each temperature. (b) Relative fluorescence of L-tryptophan in water at pH 6.7 *vs.* 1/*T*. The fluorescence intensity was normalized with respect to the value at 7°; [L-tryptophan] = 2 × 10^{-5} *M*.

van't Hoff plot of K_a in Figure 3 presents a problem as to the nature of the molecular transition which occurs with increasing temperatures. Since the temperature-dependent change occurs at the fast deprotonation step of eq 1, some steady-state equilibrium experiments were carried out at pH 8.0 where α-CT molecules would be predominantly in the A_bH_2 substate. Several small difference peaks compounded of contributions from both indole and phenol could be detected in the absorption spectra at the fixed pH of 8.0 for both α-CT and CGN A as the temperature of the sample solution was varied from 10 to 36°. Throughout this temperature range the absorbance changes for α-CT and CGN A at 293 nm, which have been used customarily and reliably as a measure of the extent of unfolding of the proteins of the chymotrypsinogen family in the thermal transition process, were zero. This shows that the extent of thermal unfolding was negligible in our experiments.

Neither a detectable change in shape of the fluorescence spectrum nor a shift in peak position was observed at pH 8.0 for both α-CT and CGN A over the temperature range from 7 to 40°.

The fluorescence yields of α-CT and CGN A at various temperatures are shown in Figure 6. For α-CT samples at least three independent experiments at each temperature were performed and the results averaged. The reproducibility of the results was better than 4%. The effect of Ca^{2+} ions on the fluorescence yield of α-CT at various temperatures was found to be negligible. This finding guarantees that the autolysis effect on α-CT samples in our measurements is insignificant since ac-

cording to Chervenka[26] Ca^{2+} ions prevent autolysis of active α-CT molecules at neutral pH values even up to 35° for periods of at least 1 hr.

The relative fluorescence yield for a protein sample was calculated choosing the quantum yield of L-tryptophan at the temperature of the sample solution as 1.00. The results as plotted in the form of relative fluorescence *vs.* $1/T$ in Figure 6 demonstrate that at both low-temperature and high-temperature ends the slopes of the curve for α-CT tend to approach limiting values while that for CGN A shows a monotonic increase with increasing temperature which may or may not be approaching a plateau at higher temperature. The temperature dependence is considerably larger than that of model indole compounds even though such compounds in polar solvents have unusually large temperature dependencies.[22] By comparison with results from model indole compounds we can conclude that the relative change in fluorescence yield is due primarily to change in the protein. Then there are three possibilities which may explain the temperature-dependent change in fluorescence of the protein system. (I) The system consists of a single species with a very large heat capacity so that over the temperature range the fluorescence changes continuously as the protein undergoes continuous change. (II) Two species with different values are present in an equilibrium which is temperature dependent. The temperature dependence of the overall fluorescence is due to changes in the relative contributions from the two species. At temperatures far removed from the transition temperature one or the other of the two species predominates and the temperature dependence of the fluorescence of the system becomes identical with that of the predominant species. (III) More than two species are in equilibrium and the fluorescence at each temperature is the net sum of contributions from the several species present at different concentrations at different temperatures.

For situation I

$$Q = q[\mathrm{P}] \tag{6}$$

$$\frac{Q}{[\mathrm{P}]} = \bar{Q} = q$$

$$\frac{d\bar{Q}}{d(1/T)} = \frac{dq}{d(1/T)} \tag{7}$$

and the observed temperature dependence of the fluorescence yield of the protein is simply the thermal quenching dependence. [P] in eq 6 is the total protein concentration of the system.

We will examine case II assuming that there are two species which are in equilibrium at pH 8.0, and consider the situation near the transition temperature (eq 8–10).

$$\mathrm{A_1} \rightleftharpoons \mathrm{A_2} \tag{8}$$

$$K = \frac{[\mathrm{A_1}]}{[\mathrm{A_2}]} \tag{9}$$

$$[\mathrm{P}] = [\mathrm{A_1}] + [\mathrm{A_2}] \tag{10}$$

[P] is the total protein concentration and K denotes the thermal-equilibrium constant of the system. Combining eq 9, 10, and 11, we obtain

$$Q = q_{\mathrm{A_1}}[\mathrm{A_1}] + q_{\mathrm{A_2}}[\mathrm{A_2}] \tag{11}$$

$$\frac{Q}{[\mathrm{P}]} = q_{\mathrm{A_1}} + \frac{(q_{\mathrm{A_2}} - q_{\mathrm{A_1}})}{K + 1} \tag{12a}$$

Tests of eq 12a can be made with our experimental results for two separate cases. In case $\mathrm{II_1}$ (shown in eq 12b) both $q_{\mathrm{A_1}}$ and $q_{\mathrm{A_2}}$ are independent of temperature, and in case $\mathrm{II_2}$ (shown in eq 12c) $q_{\mathrm{A_1}}$ and $q_{\mathrm{A_2}}$ are temperature dependent. $\Delta H_t°$ in eq 12b is the enthalpy value

$$\frac{Q}{[\mathrm{P}]} = \bar{Q}$$

$$\frac{d\bar{Q}}{d(1/T)} = (q_{\mathrm{A_2}} - q_{\mathrm{A_1}})\Delta H_t° \frac{K}{(1 + K)^2} \tag{12b}$$

associated with the thermal transition. Examination of the limiting cases for eq 12b, $K \gg 1$, $K \ll 1$, $K = 1$, shows that a plot of $\bar{Q}$ *vs.* $1/T$ should show a sigmoidal curve having symmetry with respect to the point corresponding to the transition temperature. Our results shown in Figure 6 do not conform to this picture.

$$\frac{d\bar{Q}}{d(1/T)} = \frac{dq_{\mathrm{A_1}}}{d(1/T)} + \left[\frac{dq_{\mathrm{A_2}}}{d(1/T)} - \frac{dq_{\mathrm{A_1}}}{d(1/T)}\right]\frac{1}{1 + K} + (q_{\mathrm{A_2}} - q_{\mathrm{A_1}})\Delta H_t° \frac{K}{(1 + K)^2} \tag{12c}$$

(a) For the temperature range where $A_1 \gg A_2$, $T > T_t$

$$\lim_{K \to \infty} \frac{d\bar{Q}}{d(1/T)} = \frac{dq_{\mathrm{A_1}}}{d(1/T)}$$

(b) For the temperature range where $A_2 \gg A_1$, $T < T_t$

$$\lim_{K \to 0} \frac{d\bar{Q}}{d(1/T)} = \frac{dq_{\mathrm{A_2}}}{d(1/T)}$$

(c) At the transition temperature $K = 1$

$$\lim_{K=1} \frac{d\bar{Q}}{d(1/T)} = {}^1/_2\left[\frac{dq_{\mathrm{A_1}}}{d(1/T)} + \frac{dq_{\mathrm{A_2}}}{d(1/T)}\right] + {}^1/_4(q_{\mathrm{A_2}} - q_{\mathrm{A_1}})\Delta H_t°$$

Therefore, the slope of Q *vs.* $1/T$ plot in the temperature range of a and b should approach a constant value, due to the temperature dependence of q of the species whose concentration predominates in the temperature range.

Even though our experimental results in Figure 6 do not completely rule out the possibility that case III is correct, they can be adequately explained by means of case $\mathrm{II_2}$. It is obvious from Figure 6 that the relative fluorescence change with temperature for CGN A satisfies the conditions for case I and that for α-CT is consistent with the two-state model ($\mathrm{II_2}$) and eq 12c.

Case $\mathrm{II_2}$ also specifies that the quantum efficiencies, q_i, of the two species are temperature dependent. The alternative possibility that q_i's may be independent of temperature is ruled out on the grounds that the experimental curve is not sigmoid in shape in the temperature range studied as is required in order to satisfy eq 12b for this two-state model. As is apparent in Figure 6, our results also indicate that in the temperature range of 7–40° the species predominating at the low-temperature end, $\mathrm{A_bH_2}$, has a q_i value whose temperature dependence

(26) C. H. Chervenka, *Biochim. Biophys. Acta*, 31, 85 (1959).

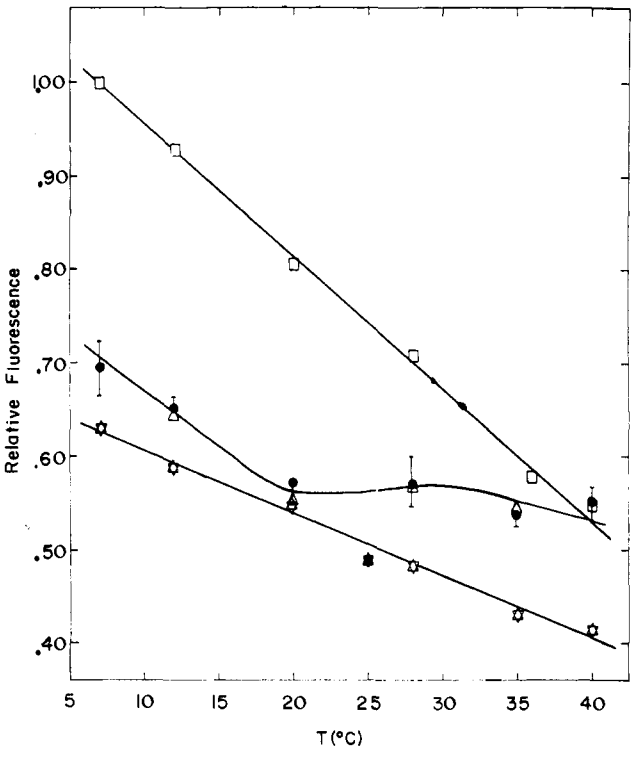

Figure 7. Relative fluorescence of L-tryptophan, α-CT, and CGN-A. The experimental conditions and the meaning of the symbols are the same as in Figure 6. (Consult the text for the procedure of obtaining this figure from the results in Figure 6.)

is the same as that of tryptophan, and therefore, the increasing temperature-dependent change in relative fluorescence of the α-CT system at high temperature is due primarily to the higher temperature species, A_fH_2. Included in Figure 6 is the relative fluorescence yield of L-tryptophan at various temperatures normalized to its value at 7°.

Making use of the values in Figure 6 one can calculate the relative fluorescence yield of α-CT and CGN A at each temperature when normalized with respect to the yield of L-tryptophan at 7°. The results are shown in Figure 7. Comparison of the temperature-dependent changes in the relative fluorescence of the three compounds, L-tryptophan, α-CT, and CGN A, clearly shows the unique, nonlinear behavior of the fluorescence change of the α-CT system in this temperature range. This point will be discussed in detail in the next section.

Discussion

The transient fluorescence change induced by pH change can be best fitted by eq 3, which is derived on the basis of formal mechanism which includes a two-proton process with a $pK_a = 18.2$. This finding might reflect a simple dimerization process in which two identical molecules bind together, but the concentration dependence of the apparent rate constant in the transient-fluorescence experiments along with the sedimentation experiments eliminate this possibility.

It is not yet established which residues in the α-CT molecule cause the change in fluorescence yield at pH 8–10. Teale and Weber[27,28] reported that the fluorescence of α-CT is due to tryptophan residues in the molecule and that tyrosine fluorescence is absent. On the basis of fluorometric titration data Cowgill[29] has concluded that ionized phenolic groups of the protein molecules function as sinks for loss of fluorescence energy of the molecules at high pH. This effect can be observed in the stopped-flow experiments when pH is perturbed to values higher than 9.8, as an initial rapid decrease in fluorescence intensity followed by a slow change of smaller magnitude. Although no details of the change in structure of α-CT with pH have been established, the drastic change in the steady-state fluorescence yield in the pH range of 8.0–9.8, where the effect of tyrosinate quenching is not significant, must be due to the readjustment of the local environment around some of the fluorescing indole side chains. A degree of cooperativity in this process for α-CT is established by the simultaneous release of two protons. This behavior established within our time resolution by the transient experiments is supported by the independent steady-state fluorescence studies which conform to the formal mechanism employed in analysis of the transients data. Our results for δ-CT are less definitive but show that the pH dependence of the rate constants for fluorescence change is closer to first order than to second order. Their common zymogen, CGN A, did not demonstrate a pH dependence of its fluorescence behavior with our sensitive fluorescence apparatus used in these experiments. The enzymically active forms of CT invariably demonstrated pH-dependent fluorescence behavior. Separation of these enzyme species into the two classes is also effected by ORD studies. Those forms having pH-dependent fluorescence properties also demonstrate pH-dependent ORD properties as shown in Table IV. The ORD changes are due primarily to changes in ellipticity in the 202- and 229-nm circular dichroism bands. Since the presence of an N-terminal α-amino group of Ileu-16 is required for the CT species to be catalytically active, one of the two ionizable groups responsible for the observed fluorescence and ORD changes may be the α-ammonium group N-terminal Ileu-16. However, the findings of Martin and Marini[30] suggest that the situation may not be explained so simply.

The relationship of the two-proton processes to "conformation change," inhibitor binding, and catalytic function will be described in a subsequent publication of this series.[31] In this paper we will simply postulate the formal mechanism shown by eq 13 in which the proton-release process marked II controls substrate binding. The kinetics of steps I and II in this mechanism are too fast to be measured with our apparatus. These steps involve considerably more change than simple ionization, as will become clear below.

$$\begin{array}{ccccccc} A_bH_2 & \rightleftharpoons & A_bH + H^+ & \rightleftharpoons & A_b + 2H^+ & \rightleftharpoons & A_c + 2H^+ \\ \uparrow\downarrow S & & \quad I \quad \uparrow\downarrow S & & \quad II & & \quad III \\ A_bH_2S & \rightleftharpoons & A_bHS + H^+ & & & & \end{array} \qquad (13)$$

Equation 13 is consistent with eq 1 and 2 and thus with our experimental results so that the slow step of the fluorescence transients is III of eq 13, *i.e.*, the conversion of substate A_b to A_c. The analysis (see Appendix) leading to eq 3 was made with data obtained at one tempera-

(27) F. W. J. Teale and G. Weber, *Biochemistry*, 65, 476 (1957).
(28) F. W. J. Teale, *ibid.*, 76, 381 (1960).
(29) R. W. Cowgill, *Biochim. Biophys. Acta*, 94, 81 (1965).
(30) C. Martin and M. Marini, personal communications, to be published.
(31) Y. Kim and R. Lumry, to be published.

ture. The analysis receives additional support from the linearity of the Arrhenius plots for k_2 and k_{-2} (Figure 3) although it will be shown elsewhere that the analysis of Arrhenius plots for some processes of enzymes like chymotrypsin is not always straightforward.[32]

The standard enthalpy and entropy changes in step III (see Table III) are much too small to be taken as evidence for significant conformation change in this process. Step II may involve the opening of the buried ion pair formed between the α-ammonium group of Ileu-16 and the carboxylate group of Asp-194. This grouping has been demonstrated in the X-ray diffraction works of Sigler, *et al.*[33] Oppenheimer, *et al.*,[5] Moon, *et al.*,[6] and Bender[3,8] have proposed that this process accompanies the proton-release process with pK_a of about 9.

The van't Hoff plot of pK_a *vs.* $1/T$ in Figure 3 demonstrates a relatively sharp curvature over the temperature range studied. Since the slowly equilibrating step of eq 2 gives a van't Hoff plot that is linear over the same temperature range, the curvature must be associated with eq 1. There are two alternative ways to describe this situation. (1) The van't Hoff plot can be divided into two linear sections and each linear section represents the enthalpic behavior of one species. In this case if the two species have small heat capacities, the slopes of the extrapolated linear sections may be used to estimate the thermodynamic functions associated with the processes at high temperature and low temperature and thence to estimate the thermodynamic difference between the species. (2) The van't Hoff plot does not consist of two lines but rather a smooth curve showing the existence of a single chemical or conformational species A_bH_2. This species has a very large heat capacity which produces the curvature. The precision and the amount of information available from Figure 3 are not sufficient to allow us to make a choice between the two descriptions. Therefore, specific studies of the nature of the thermal transition were made to test the hypotheses. With steady-state fluorescence measurements it was established that there exists a temperature-dependent equilibrium between two species of α-CT at pH 8.0, $A_bH_2 \rightleftharpoons A_fH_2$, and its transition temperature lies near 25°. In Figure 7 one can see that the temperature dependence of the fluorescence yield for α-CT is considerably different from those of L-tryptophan and CGN A, particularly in the vicinity of the transition temperature. Steiner and Edelhoch[34] reported that the thermally induced structural changes of CGN A were distinguished from the thermal quenching curve of the fluorescence similar to Figure 7 by a marked change in slope in the transition-temperature range. Our results are entirely consistent with this picture and demonstrate that a thermal equilibrium between two species is present in the temperature range studied. It has been predicted by Lumry and Biltonen[18] from their studies of its pH dependence, that the transition temperature for the thermal unfolding process of α-CT at pH 8.0 is considerably higher (>60°) than the highest temperature used in our experiments (40°). That our observations presented here are not complicated by the thermal unfolding process is established by the results of our difference-spectra experiments under comparable conditions.

The exact nature of the thermal equilibrium between A_bH_2 and A_fH_2 cannot be established until more information about this process becomes available. Nevertheless, by making use of the relationship of eq 14 and Figure 3, rough limits for some thermodynamic changes in the process can be estimated. In eq 14 A_g replaces

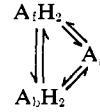

(14)

A_b as the deprotonated species of A_bH_2 and A_fH_2 for a reason which will become apparent in the later part of the discussion.

If one assumes linearity of the van't Hoff plot in the two regions of the curve, that is, $36° > t > 28°$ and $12° < t < 20°$ and extends the resulting lines to their point of intersection, the point of the sharpest curvature is found to be about 25°. Then, considering the two linear portions of the curve separately, one can estimate ΔH and ΔS for the two extreme cases: the high-temperature case and the low-temperature case. The values computed in this way are given in Table V. From

Table V. Thermodynamic Functions for the Apparent Ionization Steps $A_bH_2 \rightleftharpoons A_g + 2H^+$, $A_fH_2 \rightleftharpoons A_g + 2H^+$, Based on Mechanism 14[a]

	Temp range, °C	$\Delta H°$, kcal/mol	$\Delta S°$, eu/mol	$\Delta F°$, kcal/mol
Low-temp case (T_l) ($A_bH_2 \rightleftharpoons A_g + 2H^+$)	$t < 20$	50.6	87	24.8
High-temp case (T_h) ($A_fH_2 \rightleftharpoons A_g + 2H^+$)	$t > 28$	2.2	−76	24.5
Thermal transition ($A_fH_2 \rightleftharpoons A_bH_2$)	$t \simeq 25$	48.4	163	0.3

[a] Consult the text for this mechanism and also for the determination of the values for the thermal transition process.

eq 14 and the definitions

$$K_a = \frac{[A_g][a_H]^2}{[A_bH_2]},\quad K_f = \frac{[A_g][a_H]^2}{[A_fH_2]},\quad K_t = \frac{[A_fH_2]}{[A_bH_2]}$$

one can write the enthalpy relations for the preequilibrium state as $\Delta H_a° - \Delta H_f° - \Delta H_t° = 0$; hence, $\Delta H_t° = \Delta H_a° - \Delta H_f°$. The subscripts used here correspond to those for the equilibrium constants. For the low-temperature case, $[A_bH_2] \rightarrow [A_fH_2]$, $K_t \rightarrow 1$, and $\Delta H_{app}° \simeq \Delta H_a° = 50.6$ kcal/mol, and for the high-temperature case, $[A_bH_2] \ll [A_fH_2]$, $K_t \gg 1$, and $\Delta H_{app}° \simeq \Delta H_f° = 2.2$ kcal/mol. With these results we can estimate the thermodynamic changes in the thermal transition step, $\Delta H_t°$. The resulting values are given in the last row of Table V.

The enthalpy and entropy values for the process estimated in this way with the two-state assumption predict that conversion of one species from one state into the other should be 90% complete over the temperature interval, ΔT, of 16°. In the fluorescence curve for α-CT shown in Figure 7, if we identify the intermediate flat region where the intensity is nearly invariant with tem-

(32) C. Martin, private communication.
(33) B. W. Matthews, P. B. Sigler, R. Henderson, and D. M. Blow, *Nature (London)*, 214, 652 (1967).
(34) R. F. Steiner and H. Edelhoch, *Biochim. Biophys. Acta*, 66, 341 (1963).

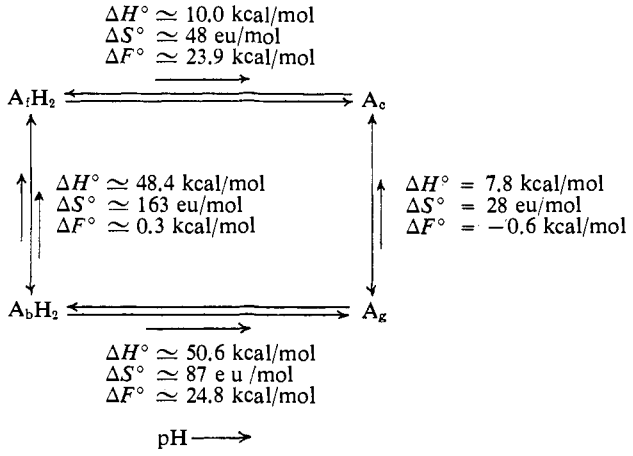

Figure 8. Schematic diagram of the thermodynamic states of α-CT at alkaline pH values.

perature as the zone of transition, the midpoint of the transition is around 25–26° and $\Delta T \simeq 12°$. One of the possibilities which can give rise to different limiting values is indicated by dotted line in Figure 3.

We can now return to the consideration of the ionization process and the subsequent changes which produce A_c as the final product. The reaction mechanism as thus far developed is described in Figure 8. The low-temperature ionization process is now written as $A_bH_2 \rightleftharpoons A_g + 2H^+$ and the high-temperature process as $A_fH_2 \rightleftharpoons A_g + 2H^+$. The thermodynamic changes estimated in the manner described above are given in Table V for both processes and for the pH-independent transition $A_bH_2 \rightleftharpoons A_fH_2$.

The qualitative similarity of the behavior of succinylated CT with CT shown in Table IV is puzzling in view of the extent of succinylation. It is possible that the α-ammonium group of Ile-16 is not succinylated by the procedure used because of its protected position. In view of the behavior of δ-CT only one acid group is necessary to explain the pH dependence in the alkaline range. Separate study of this derivative is required. The following discussion of CT does not necessarily apply to this derivative or to δ-CT.

In order to see if there is any indication of a large conformational process such as the opening of the Ile–Asp ion pair, it is necessary to make reasonable corrections for the proton-dissociation processes. The following correction procedure seems reasonable at the present time. Separate the ionization processes from the remainder thus

$$A_bH_2 \rightleftharpoons A_gH_2 \rightleftharpoons A_g + 2H^+$$

$$\underset{\text{conformation change, etc.}}{A_fH_2 \rightleftharpoons A_gH_2} \rightleftharpoons \underset{\text{ionization process}}{A_g + 2H^+}$$

The ionization step by this definition is that of solvated acid group and solvated conjugate base. Assume both acid groups are α-ammonium groups with $pK = 8$, $\Delta H_{ion}° = 11$ kcal/mol, $\Delta S_{ion}° = 0$ per group for the ionization step.[35] The results of this procedure are shown in Table VI. The enthalpy and entropy changes

Table VI. Thermodynamic Functions for the "Conformation Change" in the Apparent Ionization Step[a]

	ΔH°, kcal/mol		ΔS°, eu/mol		ΔF°, kcal/mol	
Temp limit	T_h	T_l	T_h	T_l	T_h	T_l
Overall experimental values from Table V	2.2	50.6	−76	87	24.5	24.8
Ionization of two normal NH_3^+ groups ($A_gH_2 \rightleftharpoons A_g + 2H^+$)	22[b]		0		22[b]	
Conformation change, etc.	−19.8	28.6	−76	87	2.5	2.8

[a] The values for the "conformation change" were obtained by subtracting the values for two ammonium groups from the experimental values. See the text for details. Notations T_h and T_l in this table have the same meaning as in Table V, *i.e.* T_h denotes the high-temperature case, $A_fH_2 \rightleftharpoons A_g + 2H^+$, and T_l the low-temperature case, $A_bH_2 \rightleftharpoons A_g + 2H^+$, respectively. [b] Estimated from data in ref 35.

for the "conformational" process given in the bottom row of this table are indeed quite large. If the ammonium and carboxylate groups of the Ile–Asp ion pair are disrupted in this part process, this analysis suggests that there are considerable changes in the protein in addition to changes in solvation of the charged groups. Since the species A_c is produced from A_g by increase in temperature, with $\Delta H° = 7.8$ kcal/mol, the expansion of state diagram for α-CT possible with our fluorescence data is complete. That diagram is given in Figure 1 and a schematic presentation of the estimated thermodynamic changes in the several interconversions from one A substate to another is given in Figure 8.

Our observation of curvature in the van't Hoff plot for the apparent ionization process of eq 1 has lead to the identification of the A_bH_2 and A_fH_2 substates of α-CT. The interconversion of these two substates has also been detected in experiments with substrates. Rajender, Han, and Lumry[36] found a moderate curvature centered at 25° in the plot of log k_{cat}/K_m *vs.* $1/T$ for the hydrolysis of *N*-acetyl-L-tryptophan ethyl ester in the presence of alcohol at pH 8. For the same system they have not seen any curvature in the similar plot of log k_{cat} *vs.* $1/T$. Using *N*-acetyl-L-tyrosine ethyl ester as substrate Martin[32] has observed that at pH 8 the plots of log k_{cat} against $1/T$ in water and in 3.1 *M* formaldehyde solution demonstrated sharp curvature near 21°. According to Kaplan and Laidler[37] who have reported the presence of a break in a plot of log k_{cat} *vs.* $1/T$ at 25° for the hydrolysis of *N*-benzoyl-D- and -L-alanine methyl esters, the change in the Arrhenius plot is very sharp.

The available information concerning the anomalous temperature dependence of α-CT-catalyzed hydrolysis reactions so far has not provided precise evidence as to how the $A_bH_2 \rightleftharpoons A_fH_2$ transition influences the enzymic process. This problem is further complicated by the fact that nonlinearity of the Arrhenius plots shows up in different steps of the hydrolysis reactions for different substrates.

The transition, $A_bH_2 \rightleftharpoons A_fH_2$, is essentially independent of pH at pH 8. Since the transition temperature of this process is found near 25°, under physiological conditions (37° and pH 6.5) α-CT would be expected to be predominantly in the A_fH_2 form. Rajender, Han,

(35) E. J. Cohn and J. T. Edsall, "Protein, Amino Acids and Peptides," Reinhold, New York, N. Y., 1943, pp 80–82.

(36) S. Rajender, M. Han, and R. Lumry, *J. Amer. Chem. Soc.*, **92**, 1378 (1970).

(37) H. Kaplan and K. J. Laidler, *Can. J. Chem.*, **45**, 547 (1967).

and Lumry[36] have shown that chymotryptic hydrolysis of *N*-acetyl-L-tryptophan ethyl ester proceeds nearly as well above 25° as below at this pH. Hence A_fH_2 is catalytically active at least with this substrate though the degree of relative activity is not the same. The values of the enthalpy and entropy we have estimated for the transition should not be taken very seriously. Very high experimental precision is required to estimate enthalpy changes of this type from van't Hoff plots. It is fortunate that the temperature dependence of the fluorescence from the two substates is such as to allow a distinction between a single substate with a large heat capacity and two or more substates. Our evidence is consistent with a process involving only two macroscopic states (substates A_fH_2 and A_bH_2) but the data are not yet sufficient to exclude the participation of additional substates. It should be noted that the experimental conditions of 25° and pH 8 are a very poor choice for catalytic studies with α-CT.

Appendix

Mathematical Analysis. Transient-Fluorescence Change Following a pH Change. A general two-step mechanism involving three species at least one of which has a different value of the observable is eq 1A. Our

$$A_1 \underset{w_{-1}}{\overset{w_1}{\rightleftharpoons}} A_2 \underset{w_{-2}}{\overset{w_2}{\rightleftharpoons}} A_3 \qquad (1A)$$

fluorescence-transient data require solutions consistent with a second-order proton release in step $A_1 \rightleftharpoons A_2$ or $A_2 \rightleftharpoons A_3$. Only one transient is detected with a relaxation parameter, λ, which rises with increasing pH (Figure 2). This implies that the first or the second step must equilibrate in times shorter than our maximum resolution time of about 10 msec. Hence, either $w_1 > w_2$, $w_{-1} > w_{-2}$ or $w_1 < w_2$, $w_{-1} < w_{-2}$. The protein conservation condition for our system is eq 2A. Only one

$$P = [A_1] + [A_2] + [A_3] \qquad (2A)$$

solution is consistent with these requirements. (For the complete solution of eq 1A see ref 38.) In this case $w_1 > w_2$, $w_{-1} > w_{-2}$, and $w_1 = k_1$, $w_{-1} = k_{-1}[a_H]^2$, $w_2 = k_2$, $w_{-2} = k_{-2}$. Equation 1A becomes

(38) A. A. Frost and R. G. Pearson, "Kinetics and Mechanism," Wiley, New York, N. Y., 1961, pp 175–176.

$$A_bH_2 \rightleftharpoons A_b + 2H^+ \rightleftharpoons A_c$$

and the observed relaxation constants may be expressed as

$$\lambda_1 = k_1 + k_{-1}[a_H]^2 + \frac{k_2}{1 + \dfrac{k_1}{k_{-1}[a_H]^2}} \qquad (3A)$$

$$\lambda_2 = k_{-2} + \frac{k_2}{1 + \dfrac{k_{-1}[a_H]^2}{k_1}} \qquad (3B)$$

The relaxation parameter λ_1 is too large to be measured with the stopped-flow method. Hence λ_2 of eq 3B is the required relaxation parameter. This conclusion is quantitatively consistent with all the observations reported in this paper and has been used throughout. We let $k_{-1}/k_1 = 1/K_a$ and q_i be the intrinsic fluorescence yield using eq 3B as given by eq 4B along with eq 5A and 6A. At $t = 0$, $[A_b] = [A_b]_0$, $[A_c] = [A_c]_0$, and $Q(t) =$

$$Q(t) = q_{A_bH_2}[A_bH_2] + q_{A_b}[A_b] + q_{A_c}[A_c] \qquad (4A)$$

$$Q(t) = Q(0) + \delta(1 - e^{-\lambda_2 t}) \qquad (4B)$$

$$Q(0) = q_{A_bH_2}[P] + (q_{A_b} - q_{A_bH_2})[A_b]_0 + (q_{A_c} - q_{A_bH_2})[A_c]_0 \qquad (5A)$$

$$\delta = (q_{A_b} - q_{A_bH_2})\left[\frac{k_{-2}[P]}{k_2 + k_{-2}\left(1 + \dfrac{[a_H]^2}{K_a}\right)} - [A_b]_0\right] + (q_{A_c} - q_{A_bH_2})\left[\frac{k_{-2}[P]}{k_2 + k_{-2}\left(1 + \dfrac{[a_H]^2}{K_a}\right)} - [A_c]_0\right] \qquad (6A)$$

$Q(0)$.

Steady-State Fluorescence Yield. From eq 4B, $Q(\infty) = Q(0) + \delta$, which yields eq 7A. In all these

$$\frac{Q(\infty)}{[P]} = \frac{q_{A_bH_2}[a_H]^2 + q_{A_b}K_a + q_{A_c}(k_2/k_{-2})K_a}{[a_H]^2 + K_a + (k_2/k_{-2})K_a} \qquad (7A)$$

equations the hydrogen-ion activity is that of the final solution since hydrogen ions are released only in the rapid preequilibrium step $A_bH_2 \rightleftharpoons A_b + 2H^+$, K_a.